

## Supporting Information

# **Largely Enhanced Electromagnetic Wave Absorption via surface coating of Carbonyl Iron Particle by Liquid Metal**

Kang Xie, Qin Zhang\*, Feng Chen \*, and Qiang Fu

College of Polymer Science & Engineering, State Key Laboratory of Polymer Materials Engineering, Sichuan University, Chengdu, 610065, P. R. China.

\* Corresponding author. E-mail: qinzhang@scu.edu.cn (Qin. Zhang); fengchen@scu.edu.cn (Feng. Chen)

## Supplementary Fig.s and Tables

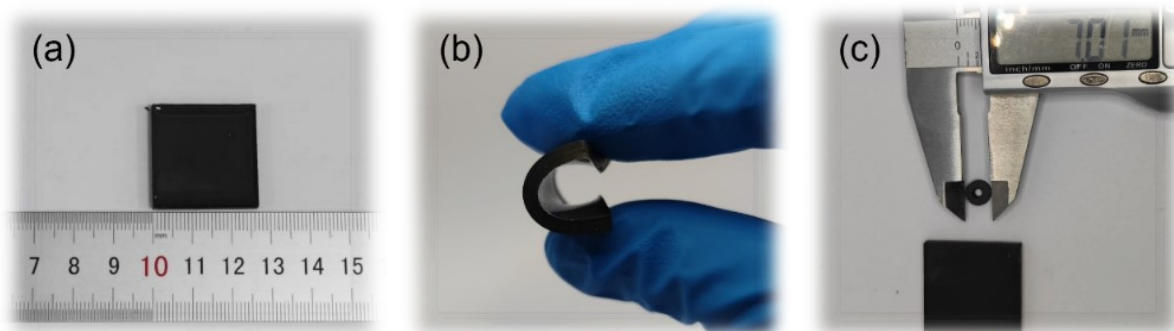


**Fig. S1** (a) Schematic of CIP@LM-PDMS. (b) Demonstration of the flexibility of CIP@LM-PDMS. (c) Sample for testing the electromagnetic parameters of CIP@LM-PDMS.

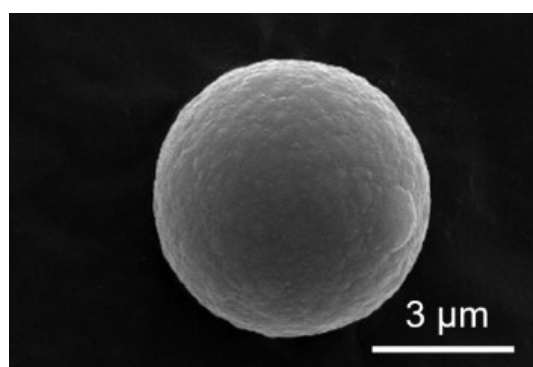


**Fig. S2** Scanning electron microscopy (SEM) image of CIP.

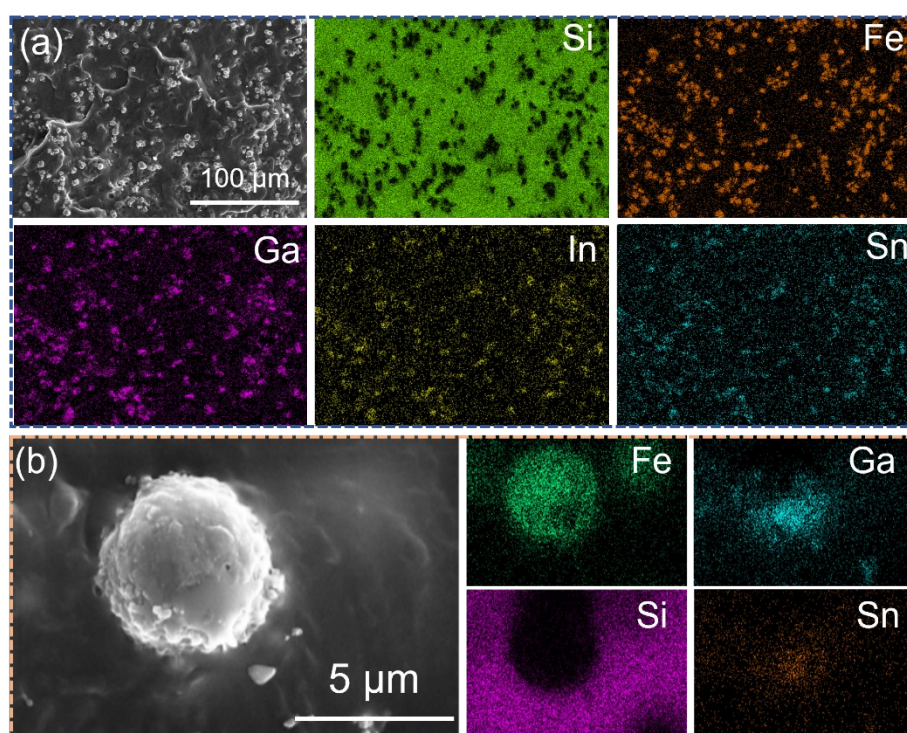


**Fig. S3** (a, b) SEM images and elemental mapping of CIP@LM-PDMS.

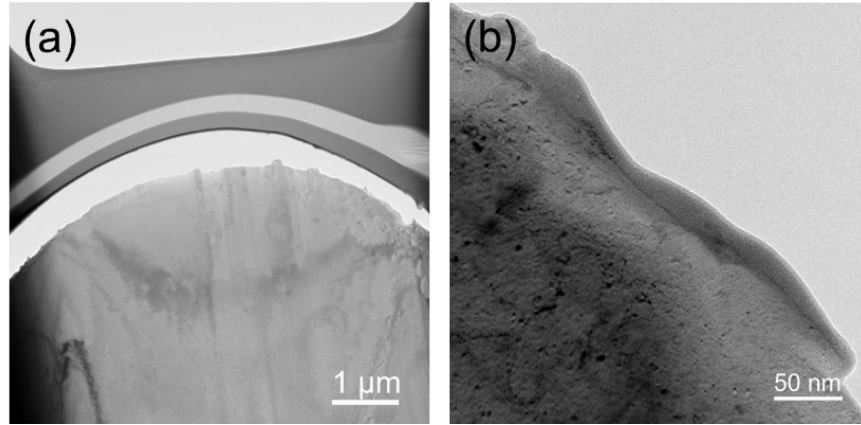


**Fig. S4** (a, b) Transmission electron microscopy (TEM) images of CIP@LM cross-sectioned with a focused ion beam.

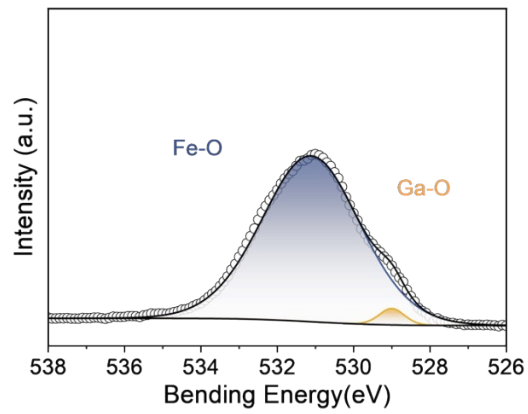


**Fig. S5** X-ray photoelectron spectroscopy O1s spectra of CIP@LM composite.

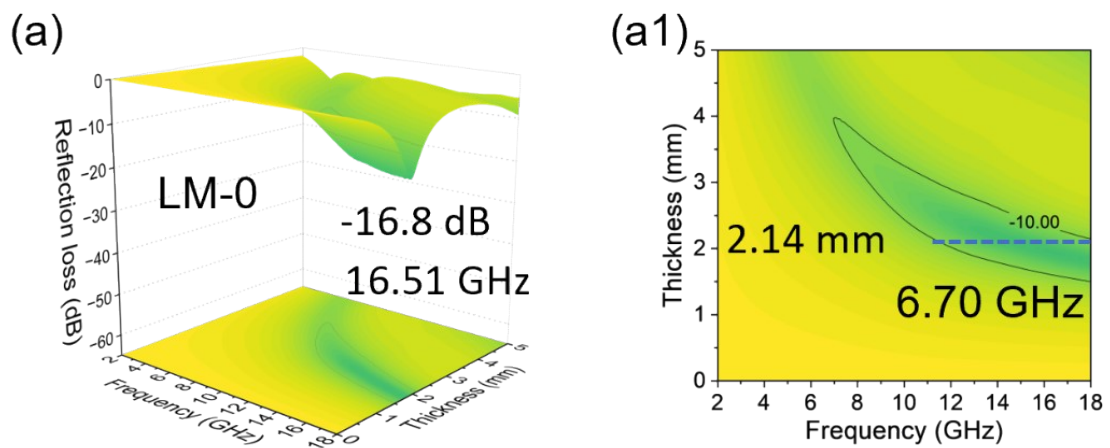


**Fig. S6** (a, a1) Electromagnetic wave absorption properties of CIP (LM-0) depicted through three-dimensional and two-dimensional reflection loss (*RL*) maps.

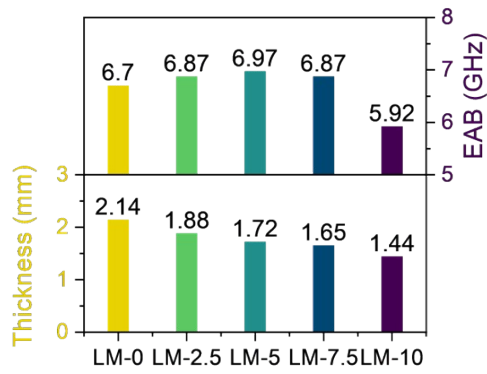


**Fig. S7** Bar charts representing the microwave absorption bandwidth (EAB) of CIP@LM.

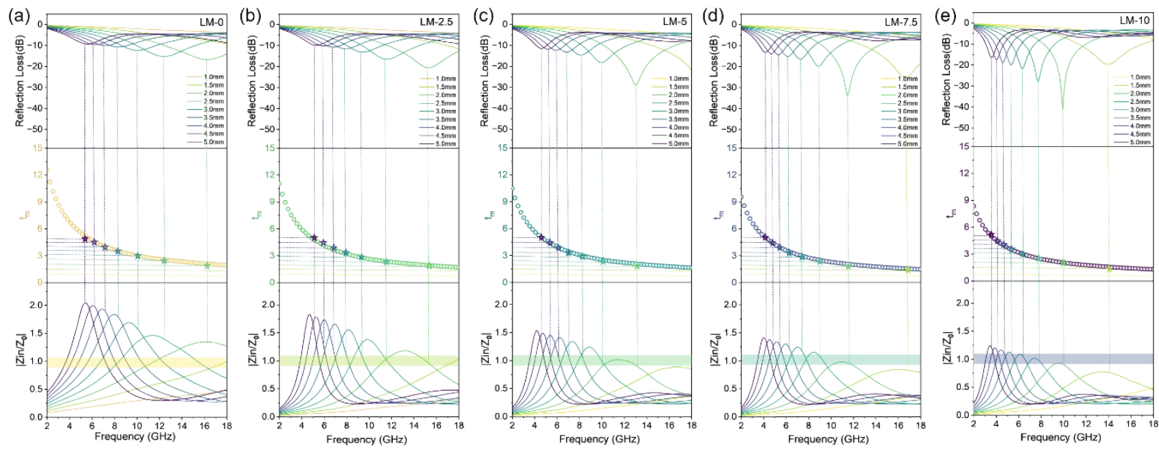


**Fig. S8** RL as a function of matched thickness and frequency at a quarter-wavelength ( $\lambda/4$ ) and impedance matching characteristics for (a) LM-0, (b) LM-2.5, (c) LM-5, (d) LM-7.5, and (e) LM-10.

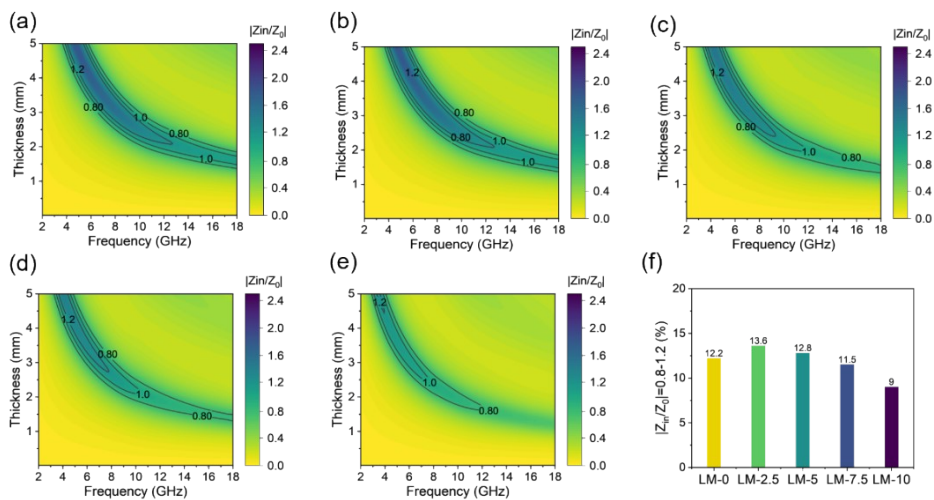


**Fig. S9** Impedance matching degree maps  $|Z_{in}/Z_0|$  for (a) LM-0, (b) LM-2.5, (c) LM-5, (d) LM-7.5, and (e) LM-10. (f) Ratio of  $|Z_{in}/Z_0|$  values within the range of 0.8-1.2.

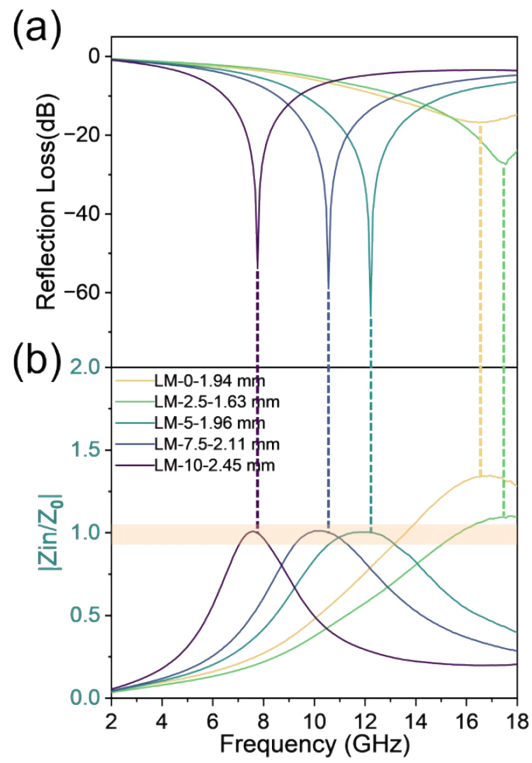


**Fig. S10** (a) Minimum  $RL$  value and corresponding thickness. (b) Impedance ( $Z$ ) values of CIP@LM.

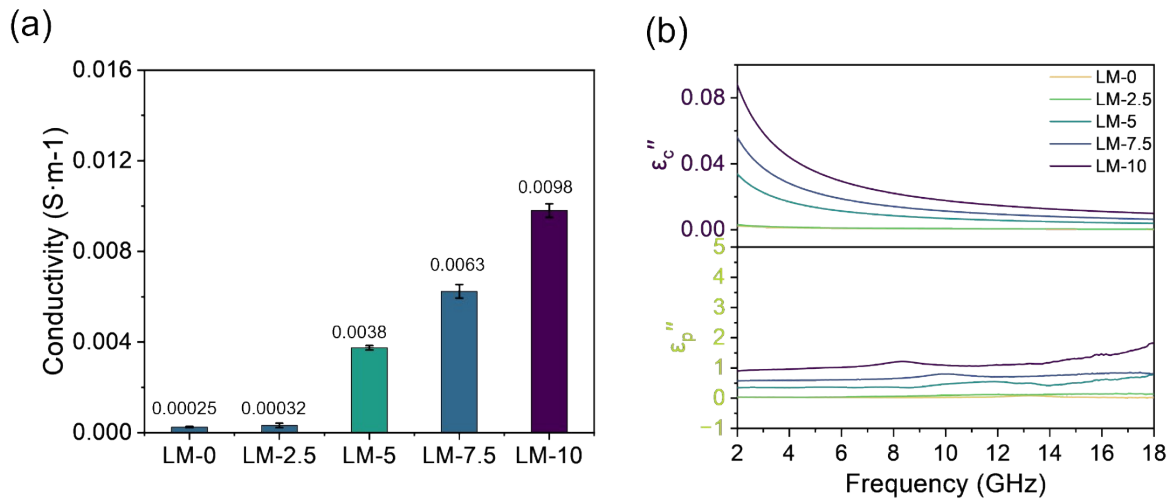


**Fig. S11** (a) Electrical conductivities, (b)  $\epsilon_c''$  and  $\epsilon_p''$  of LM-0, LM-2.5, LM-5, LM-7.5, and LM-10.



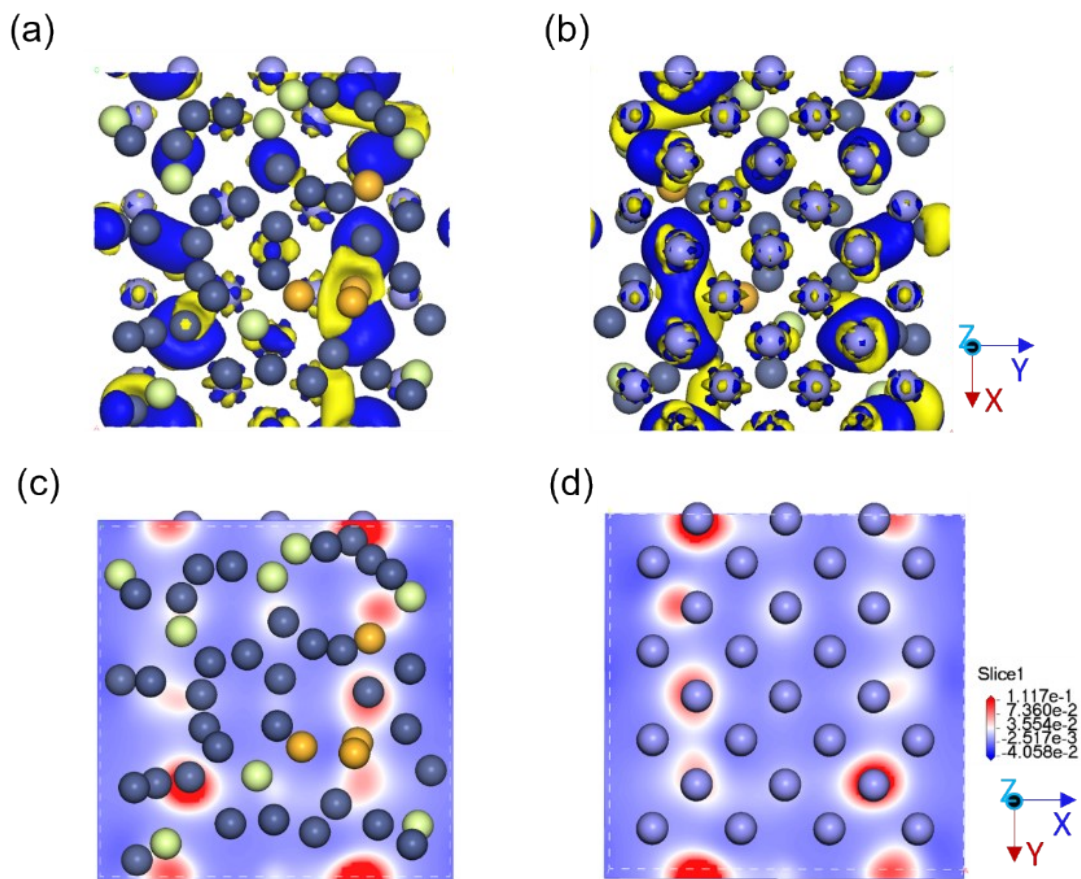


**Fig. S12** (a, c) Differential charge density of CIP@LM from an upward perspective. (b, d) Top view of the differential charge density of CIP@LM.

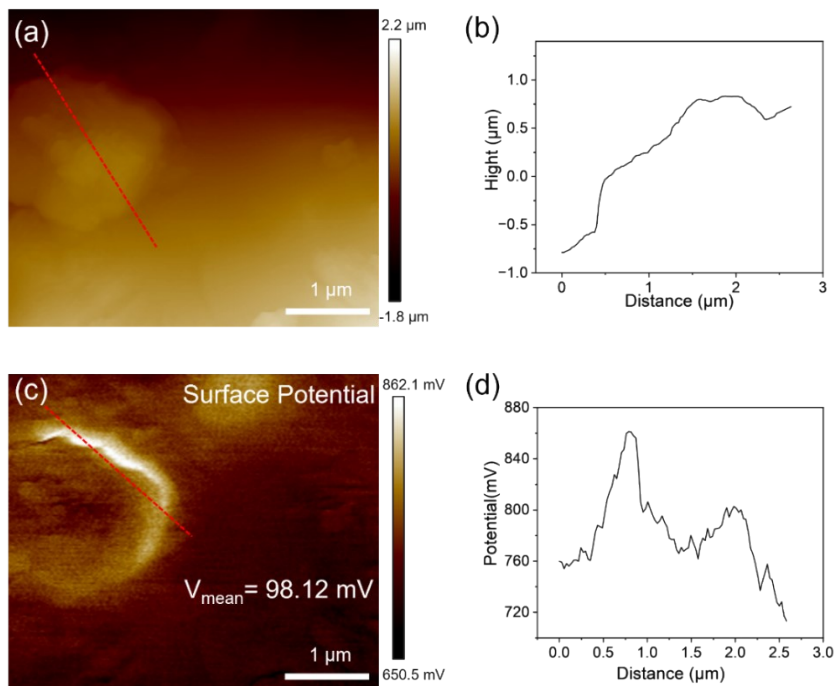


**Fig. S13** (a, b) Atomic force microscopy (AFM) and height profile images of LM-5. (c, d) Kelvin Probe Force Microscopy (KPFM) data for LM-5.

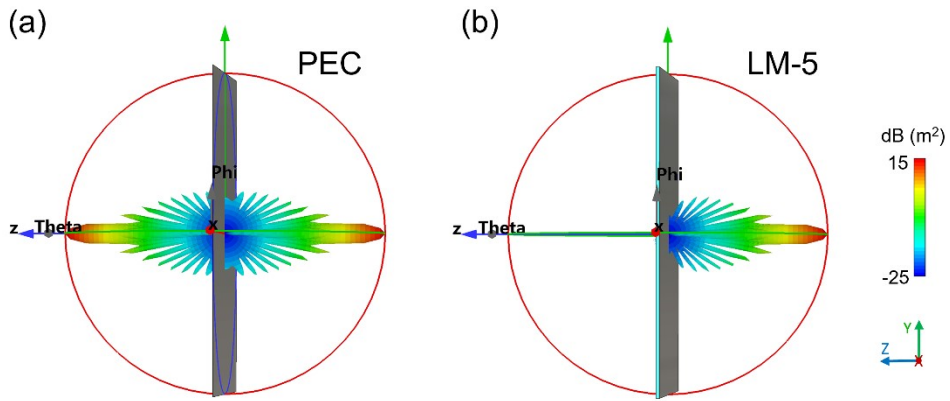


**Fig. S14** (a, b) 3D diagrams of radar cross section (RCS) simulations for the perfect electric conductor (PEC) (0.1 mm) and LM-5 (1.96 mm) at 12.22 GHz.

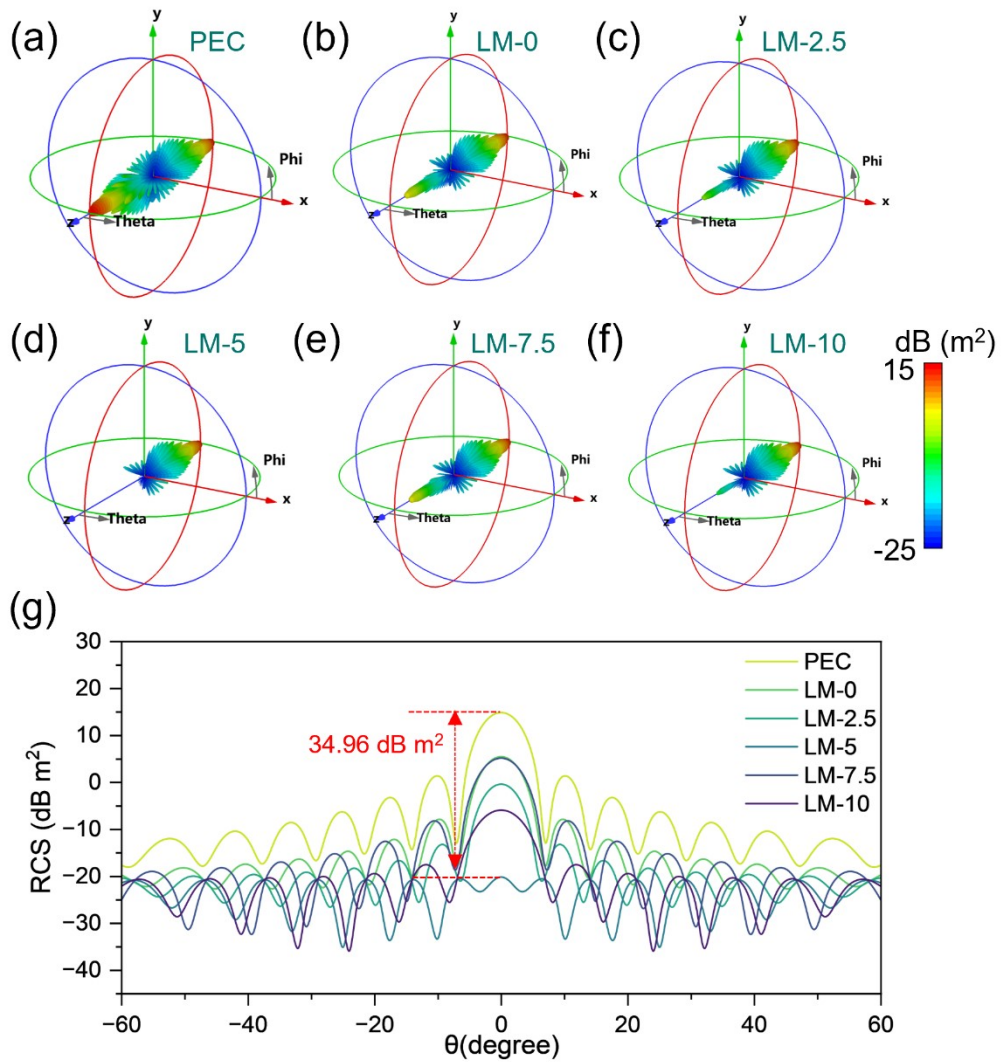


**Fig. S15** (a–f) 3D radar wave scattering signals for all samples. (g) RCS values for all samples.

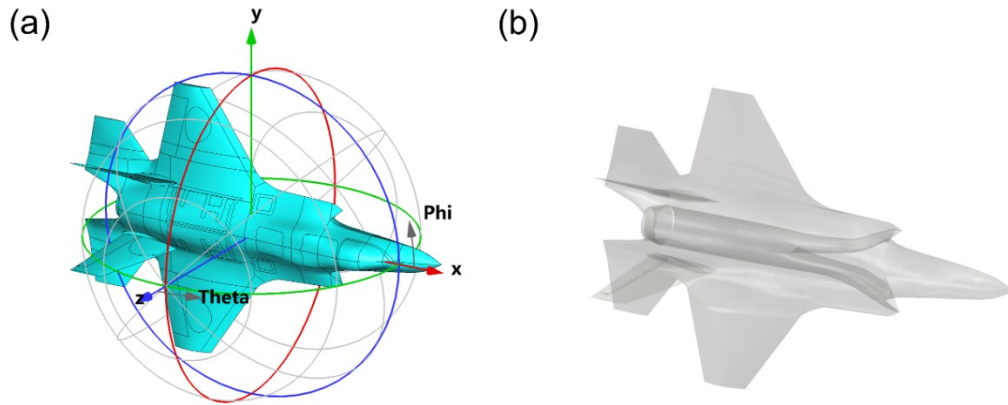


**Fig. S16** (a) RCS simulation of F35 in CST Studio Suite 2022. (b) Location of stealth coating on the fighter aircraft.

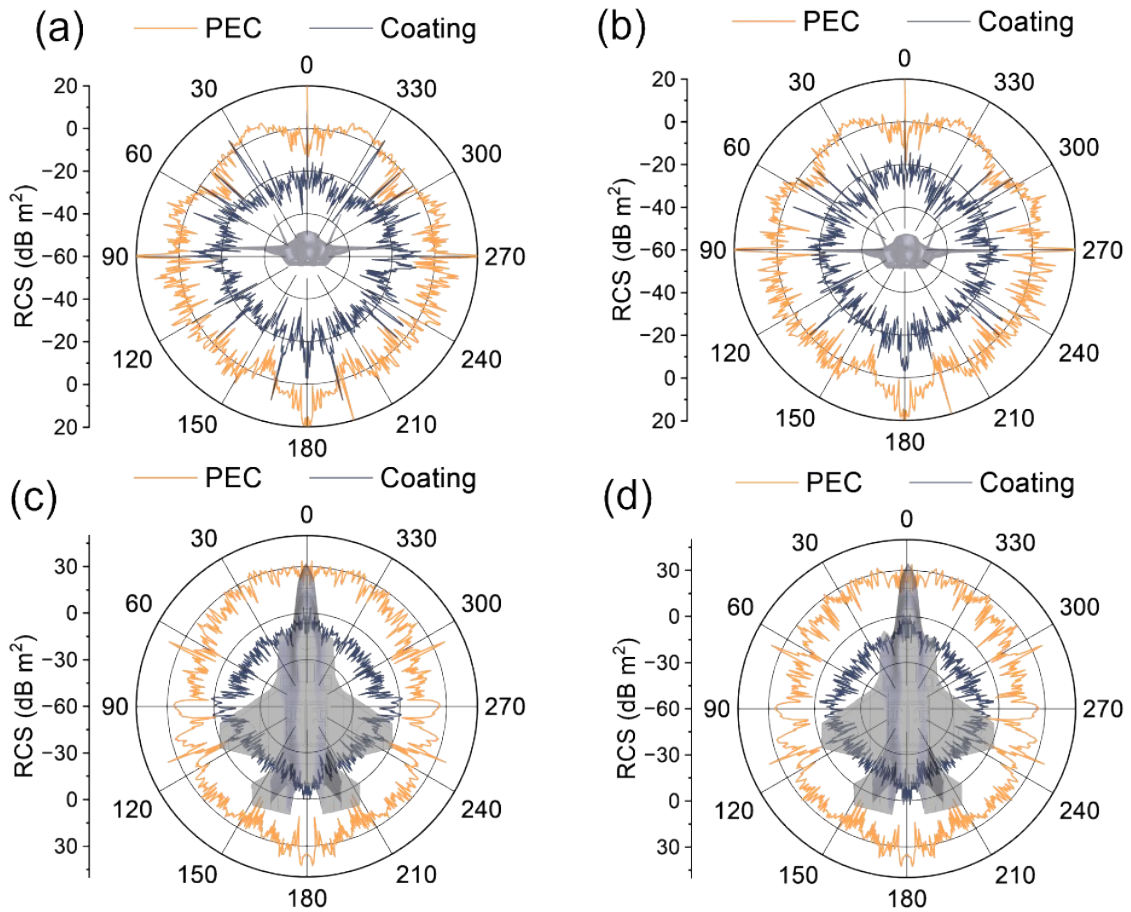


**Fig. S17** (a, b) Forward view RCS of the fighter aircraft at 12.22 GHz for horizontal and vertical polarization, respectively. (c, d) Top view RCS of the aircraft at 12.22 GHz for horizontal and vertical polarization, respectively.



**Table S1.** Comparison of  $RL_{min}$  and EAB among reported absorbers for electromagnetic wave absorption

Absorbers	$RL_{min}$ (dB)	EAB (GHz)	Reference
CIP@SiO <sub>2</sub> @NC	-25.7 dB	6.9 GHz	1
Cr <sub>5</sub> Te <sub>8</sub> @GNS	-57.6dB	4.4GHz	2
Cu@LM	-39.6dB	4.96GHz	3
CoS <sub>2</sub> @GNS	-51.9dB	4.8	4
Ni@Ga	-55.9	3.92	5
NiFe <sub>2</sub> O <sub>4</sub> @PPy	-51.3	6.8	6
N-Ni@C	-59.56	6	7
CoNi@PNPs	-59.9	6.82	8
PPy@RGO@LM	-46.81	4.5	9
CIP@GO	-56.4	5.1	10
NiFe <sub>2</sub> O <sub>4</sub> @GNS	-48.1	5.3	11
CIP@LM	-65.9	6.96	This work

## Supporting references

- 1 W. Dai, F. Chen, H. Luo, Y. Xiong, X. Wang, Y. Cheng and R. Gong, *J. Alloys Compd.*, 2020, **812**, 152083.
- 2 L. Qin, Z. Guo, S. Zhao, D. Kong, W. Jiang, R. Liu, X. Lv, J. Zhou and Q. Shu, *Nano-micro Lett.*, 2023, **16**, 60.
- 3 Y. Wang, Y. N. Gao, T. N. Yue, X. D. Chen, R. Che and M. Wang, *J. Colloid. Interface. Sci.*, 2022, **607**, 210-218.
- 4 J. Ding, R. Shi, C. Gong, C. Wang, Y. Guo, T. Chen, Y. Zhang, H. Cong, C. Shi and F. He, *Adv. Funct. Mater.*, 2023, **33**, 2305463.
- 5 B. Zhao, Y. Du, H. Lv, Z. Yan, H. Jian, G. Chen, Y. Wu, B. Fan, J. Zhang, L. Wu, D. W. Zhang and R. Che, *Adv. Funct. Mater.*, 2023, **33**, 2302172.
- 6 L. Rao, Z. Li, Y. Qian, M. Huang, L. Wang, Y. Liu, J. Zhang, Y. Lai, C. Liang and R. Che, *Chem. Eng. J.*, 2024, **488**, 150955.
- 7 Y. Pan, Q. Zhu, J. Zhu, Y. Cheng, B. Yu, Z. Jia and G. Wu, *Nano Res.*, 2023, **16**, 10666-10677.
- 8 L. Rao, Z. Liu, L. Wang, W. You, C. Yang, R. Zhang, X. Xiong, L. Yang, H. Zhang, J. Zhang, H. Lv and R. Che, *Adv. Funct. Mater.*, 2023, **33**, 2306984.
- 9 L. Wang, L. Huang, Y. Li and Y. Yuan, *J. Appl. Phys.*, 2022, **132**, 19.
- 10 S. Jeon, J. Kim and K. H. Kim, *J. Appl. Surf. Sci.*, 2019, **475**, 1065-1069.
- 11 Y. Wang, Y. N. Gao, T. N. Yue, X. D. Chen, R. Che and M. Wang, *J. Colloid. Interface. Sci.*, 2022, **607**, 210-218.